BUILDING RESEARCH JOURNAL
VOLUME 60, 2012 NUMBER 3 – 4

FAILURE PROCESS OF CARBON FIBER COMPOSITES

ALEXANDER TESAR

Some research results of failure behaviour of carbon fiber composites are presented. The solution of material instability on the basis of fiber kinking theory is adopted for the treatment of the failure process. The micromechanical modeling adopting the FETM-approach is used for a numerical analysis of the problem. Some numerical and experimental results with an actual application are submitted in order to demonstrate the efficiency of the approaches suggested.

Keywords: FETM-approach, fiber kinking, carbon fiber composite, failure process, material instability, transformaton strain, ultimate behaviour

1. Introduction

A multilevel approach for the local micromechanics analysis of carbon nanotube based composite materials is suggested. Carbon nanotubes are seen as graphene sheets rolled into hollow cylinders composed of hexagonal carbon cells. The hexagonal cell is repeated periodically and binds each carbon atom to three neighboring atoms with covalent bonds, creating one of the strongest chemical bonds today, with impressive mechanical properties.

A long-standing difficulty in designing the carbon fiber composites is the formulation of a consistent theory that describes their failure behaviour under nonuniform stress fields. There is a problem of discrepancy between the four-point bend and simple tensile test data that might appear. The bend specimens fail at a higher strain compared with the tensile specimens. When the bend and tensile data are analysed using a classical linear elastic theory the bend stress at any strain prior to failure of a tensile test specimen is 20 – 35 % higher than the corresponding uniaxial tensile stress. Such strength discrepancy remains unresolved even when corrections are made for the nonlinearity of the stress-strain curves. By attempts to explain such discrepancy only very limited success has been achieved with failure theories, including the Weibull`s statistical model and the fracture mechanics approach. Similar experiences also appeared by the application of linear fracture mechanics or couple-stress theory.

The carbon fiber composites adopted in present structural engineering are made of typical components listed as:

1. carbon fibers, with strength and elasticity moduli in scope 2.2 – 5.7 GPa and 300 – 700 GPa, respectively,
2. aramide fibers, with strength 3.5 GPa and elasticity moduli in scope 80 – 185 GPa.

Institute of Construction and Architecture, Slovak Academy of Sciences, Dubravska cesta 9, 845 03 Bratislava, Slovak Republic, e-mail: alexander.tesar@savba.sk

The carbon fiber composites consist of micromechanical fibers and surface resin skin. The calculation on the micromechanical level takes into account the behaviour of a single fiber in interaction with other fibers and with surface skin. In present time there are available new types of fiber composites equipped with surface skin on the basis of advanced ceramics or metals having a high strength and load-bearing capacity as well as increased temperature resistance and fatigue reliability.

The material instability appearing in the failure process of carbon fiber composites is treated by the fiber kinking theory using the analysis on the micromechanical level. In this paper the following is submitted:

1. fiber kinking approach for the failure analysis of carbon fiber composites,
2. mathematical formulation of governing equations for modeling and numerical treatment of the problem,
3. numerical and experimental assessment with structural application.

2. Analysis

In carbon fiber composites the transformation strains and other field quantities appearing in elastic moduli are periodic functions of space, time and temperature. The periodicity is exploited in an effort to obtain accurate estimates for the transformation strains used to approximate mechanical properties of such composites.

The Washizu´s variation principle is adopted in order to include initial stress and strain components into analysis. The stress in the carbon fiber microelement at the beginning of time and temperature increments studied is considered as an initial stress with thermal strain increments. The variation principle under consideration is then written in the terms of time rate quantities given by

$$I = \{\int_V [S_{ij}\,\varepsilon_{ij} + 0.5\,W_{ij}\,u_{ki}\,u_{kj} - (\varepsilon^{o}_{ij} + 0.5\,\varepsilon'_{ij})\,S_{ij}]\;dV - \int_{A1} r_i\,u_i\,dA1 - \int_{A2} s_i\,(u_i - w_i)\,dA2\}(dt)^2$$

$$+ \{\int_V W_{ij}\,\varepsilon_{ij}\,dV - \int_{A1} r_i\,u_i\,dA1 - \int_{A2} p_i\,(u_i - w_i)\,dA2\}dt\,, \tag{1}$$

where W_{ij} and S_{ij} are the Piola-Kirchhoff stress tensors for initial stress and strain rate states, respectively, p_i and s_i are the Lagrangian surface traction and its time rate quantity, respectively, r_i and $r_i^{(.)}$ are prescribed on the surface area $A1$ and w_i on the area $A2$ and $\boldsymbol{V}$ is the volume bounded by the surface area $A=A1+A2$. The total strain rate ε_{ij} is composed of the initial strain rate ε^{o}_{ij} and ε'_{ij}, corresponding to the instantaneous stress rate S_{ij}. To evaluate the thermal strain rate the thermal expansion coefficient at temperature T is α(T) and at temperature T+dT is α(T+dT). By expanding α(T+dT) into Taylor series the average thermal strain rate is obtained. The governing equation is given by

$$\mu\,\eta(w_t) + (\lambda + \mu)\,\mathrm{grad}(\mathrm{div}\,w_t) + f = \rho\,\partial^2 w_t/\partial t^2\,, \tag{2}$$

where λ and μ are Lame´s constants, the density is ρ, the corresponding Laplace operator is η, the body force vector is f and the vector of displacements is w_t (Tesar and Svolik, 1993).

In the terms of derivatives of displacements w_t the governing equation is given by

$$c_2\,w_t + (c_1^2 - c_2^2)\,w_t + f_i/\rho = a_t\,, \tag{3}$$

with propagation velocities for dilatational displacements

$$c_1 = \sqrt{[(\lambda + 2\mu)/\rho\ ]}, \tag{4}$$

and shear displacements

$$c_2 = \sqrt{(\mu/\rho)}\ . \tag{5}$$

Strain and stress components are given by

$$\varepsilon_{ij} = (w_{i,j} + w_{j,i})/2 \tag{6}$$

and

$$\sigma_{ij} = \lambda\ \varepsilon_{kk}\ \delta_{ij} + 2\ \mu\ \varepsilon_{ij},\ i,j = 1, 2, 3, \tag{7}$$

with Kronecker delta function δ_{ij} .

3. Failure process

The kinking of microscopic fiber bundles focuses the attention on this type of material instability when dealing with the failure process of carbon fiber composites. The material buckling of carbon fibers under static or dynamic compression and flexure is assumed as a possible mode of failure as well as the item influencing the above bend/tensile discrepancy. The local short-wave imperfections as well as general long-wave imperfections along the length of fibers (Budiansky, 1983) are to be taken into account.

An elastic plane strain inextensional deformation in compressed part of the carbon fiber composite gives displacements $w(x,y)$ in normal direction to the fibers, governed by

$$(1 - \sigma/G)\ \partial^2 w/\partial x^2 + E_T/G\ \partial^2 w/\partial y^2 = (\sigma/G)\ \partial^2 w_o/\partial x^2\ , \tag{8}$$

where $w_o(x,y)$ is an initial displacement pattern. Taking into account the half-plane $y \geq 0$ the effect of a short-wave imperfection is given by

$$w_o = \delta_D(x)\ \delta_D(y)\ , \tag{9}$$

where δ_D is the symbol for the Dirac delta function.

A long-wave imperfection concentrated at the edge $y = 0$ is given by

$$w_o = -\ |\ x\ |\ \delta(y)\ . \tag{10}$$

The deviations from ideal fiber alignment due to the fiber spacing irregularities induce the patterns of angular misalignment (elastic distortion) that arrange themselves into inclined domains. Such rotations induce the plastic kinking into similarly inclined kink bands. The failure follows there after the start of plastic deformation with kinking failure stress σ_s.

The consequent correlations between σ_s and kink angle β for long wave imperfections (see Fig. 1) are given by

$$\tan \beta = \pm \sqrt{[(1 - \sigma_s/G)/(E_T/G)]} \tag{11}$$

and for short wave imperfections by

$$\tan \beta = \pm (\sqrt{(2)} - 1) \sqrt{[(1-\sigma_s/G)/(E_T/G)]}. \tag{12}$$

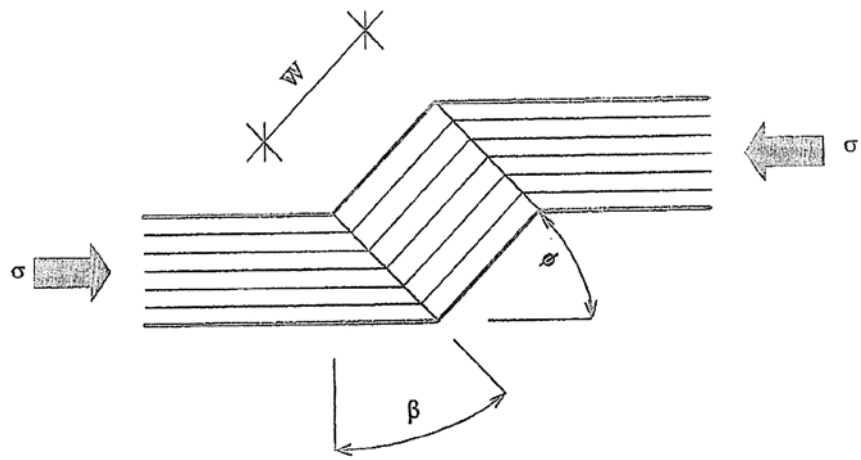

Figure 1. Kinking of fiber bundles

To find rational estimates for the kink width W (see Fig. 1) the single fiber dimensions are to be taken into account. The carbon fiber diameter d is the meaningful size in the problem. The kink width is clearly delineated by bending in the fibers so that the local fiber bending resistance must be considered explicitly. The fibers are assumed to undergo inextensional bending until they break. At the same time, the elastic strain in the matrix can be neglected with respect to its plastic strains, i.e., the matrix is assumed to be rigid-plastic. Smoothing of the fibers then states a simple couple-stress formulation which gives no fiber rotations outside a band. The rotation $\phi(x + y \tan \beta)$ within the band is governed by

$$d^2\phi/dX^2 + \sigma/\tau_r = 1 , \tag{13}$$

with

$$\tau_r = (\tau_y^2 + \sigma_{Ty}^2 \tan^2 \beta)^{1/2} \text{ and } X = (4x/d) [\tau_r /(c E)] \tag{14}$$

and with c as the volume concentration of carbon fibers.

By treatment of Eq. (13) with the condition that the rotations vanish at the ends of the kinking domain, the evolution of the plastic kinking is studied. The carbon fiber breaking is presumed to

occur when a critical tensible strain ε_F is reached in combined compression and flexural action at the points of the maximum curvature. For the case of perfectly brittle fibers then the formula pays for the kink width given by

$$W/d = \pi/4\ [(2\ \tau_{ry})/(c\ E)]^{-1/3}\ . \tag{15}$$

The equation holds for perfectly straight fibers. However, the studies that take initial misalignment into account have shown that W can substantially differ from the perfect fiber case. An idea appears there to adopt the micromechanical simulation of single fibers by micro strings in order to study the problem. The resistance of such single string fibers contains elastic, plastic, visco-elastic and visco-plastic parameters possibly appearing (Simo, 1990). One approach for such a model is submitted below.

For physical interpretation of the above definitions the internal and left-hand external displacements of one string microelement are denoted by w_a and w_b. The internal displacement vector w_i is eliminated beforehand, giving the stiffness matrix by

$$K(\omega) = \begin{bmatrix} K_{aa} & K_{ab} \\ K_{ba} & K_{bb} \end{bmatrix}, \tag{16}$$

and the deformation vector by

$$w = \begin{bmatrix} w_a \\ w_b \end{bmatrix}. \tag{17}$$

Corresponding force vectors are given by

$$n_a = K_{aa}\ w_a + K_{ab}\ w_b\ , \tag{18}$$

$$n_b = -\ K_{ba}\ w_a - K_{bb}\ w_b\ . \tag{19}$$

The state vector v is defined as the combination of displacements and internal forces given by

$$v = [w, n]^T\ . \tag{20}$$

The state vector at the boundaries a and b is given by

$$v_b = S\ v_a\ , \tag{21}$$

with the corresponding transfer matrix S. It holds

$$S = \begin{bmatrix} S_{aa} & S_{ab} \\ S_{ba} & S_{bb} \end{bmatrix}, \tag{22}$$

with

$$S_{aa} = -K_{ab}^{-1}\ K_{aa}\ ,\ S_{ab} = K_{ab}^{-1}\ ,\ S_{ba} = -K_{ba} + K_{bb}\ K_{ab}^{-1}\ K_{aa}\ ,\ S_{bb} = -K_{bb}\ K_{ab}^{-1}\ . \tag{23}$$

The damping parameters are partially contained in the isothermal bulk modulus K_I given by

$$K_I = K_o(1 + i\,\eta_B) \tag{24}$$

and appearing in the stiffness terms of the transfer matrix S. In Eq. (24) η_B is the damping factor.

The heterogeneity is an essential ingredient of the thermoelastic dissipation in the body of the carbon fiber composites studied. The adiabatic bulk modulus K_A is related to the isothermal modulus K_I by

$$K_A = K_I\,[\,1 + K_I\,\gamma^2\,T/C_V\,], \tag{25}$$

where γ is the volumetric thermal expansion coefficient, C_V is the heat capacity at the constant volume and T is the absolute temperature.

The increased stiffness under adiabatic conditions is due to the fact that compression produces heating and therefore more pressure is needed to produce the given volumetric strain compared with isothermal conditions. In carbon fiber composite the adiabatic heating induce nonuniform temperatures under oscillatory loading and the heat will then flow among the constituents. The consequent phase difference between the stress and strain leads to energy dissipation in each stress cycle.

The velocity v versus stress σ is then given by

$$v = \rho/G + \sigma/\eta\,, \tag{26}$$

with ρ as the time differentiation of σ. Considering the substitution $\upsilon = G/\eta$ and taking into account the initial conditions $\nu(0) = 0$ and $\sigma(0) = 0$ for $t = 0$, the average stress is given by

$$\sigma_a = G \int e^{-\upsilon(t)}\,a(t)\,dt\,, \tag{27}$$

with acceleration $a(t)$.

With the spectral function $N(\upsilon)$, specifying the density of υ and G in the microelement carbon fiber spring studied, the resulting stress is given by

$$\sigma_R = G_o\,v + \int N(\upsilon)d\upsilon \int e^{-\upsilon\,t}\,a(t)\,dt\,. \tag{28}$$

Adopting the value

$$G_s = \int N(\upsilon)\,d\upsilon\,, \tag{29}$$

as well as the function of relaxation

$$\Psi(t) = G_s(1 - G_s^{-1} \int N(\upsilon)\,e^{-\upsilon t}\,d\upsilon)/(G_o+G_s)\,, \tag{30}$$

the resulting stress is modified into

$$\sigma_R(t) = (G_o+G_s)\,[v(t) - \int a(t)\,\Psi(t)\,dt\,]. \tag{31}$$

For the approach of $N(\upsilon)$ the Dirac function given by $\delta(x) = 0$ for $x \neq 0$ and by $\int \delta(x)\,dx = 1$ is adopted. Because for each function $f(x)$ there holds

$$\int f(x)\,\delta(x - x_o)\,dx = f(x_o)\,, \tag{32}$$

the approach required may be done by replacing the function $\upsilon\, e^{-\upsilon t}$ by substitution $t^{-2}\,\delta(\upsilon - t^{-1})$. The approximation for $N(\upsilon)$ is then given by

$$N(\upsilon) \approx \upsilon^{-1}\,\Psi(1/\upsilon)\,. \tag{33}$$

Adopting the above analysis the complex modulus of elasticity, appearing as a function of the frequency ω, is given by

$$E = G_o + i\omega \int N(\upsilon)/(\upsilon + i\omega)\,d\upsilon\,. \tag{34}$$

The division into real and imaginary components then yields

$$E_1 = G_o + \int \omega^2/(\omega^2 + \upsilon^2)\,N(\upsilon)\,d\upsilon \tag{35}$$

and

$$E_2 = \int \omega\upsilon/(\omega^2 + \upsilon^2)\,N(\upsilon)\,d\upsilon\,, \tag{36}$$

with G_o valid for $\omega = 0$.

Instead of infinite number of microelements the above approach allows the modeling of the carbon fiber material by string elements with modulus $G(\omega)$ and stiffness $\eta(\omega)$, both appearing as functions of the frequency ω. The complex modulus of elasticity is then given by

$$E = G(\omega) + \eta(\omega)\,\omega i \tag{37}$$

and is implemented into the stiffness terms of corresponding complex transfer matrix *S*.

The calculation run of the FETM-wave approach (Finite Element versus Transfer Matrix Methods), using the above matrix S, is adopted with updated variability of micromechanical mesh size in space, time and temperature. The details of the approach are summed up in (Tesar and Fillo, 1988) or in (Tesar and Svolik, 1993). Adopting the approach the ultimate analysis of carbon fiber elements is given by

1. Micromechanical modeling of the material and macromechanical modeling of the structural configuration in space, time and temperature.
2. Updated calculation of stress and strain in space, time and temperature.
3. Automatic comparison with ultimate strength of the elements adopted.
4. Initiation of cracks in micromechanical elements trespassing the ultimate strength.
5. Updated calculation of the crack distribution in space, time and temperature until total failure of structure.

The regime of the crack initiation and distribution is rather complex. One or several cracks develop and propagate slowly along the critical regions of the carbon fiber material studied. In case of the shear the cracks turn inside of the body in a direction being quasi-perpendicular to the tension.

4. Numerical and experimental verification

Numerical and experimental assessment of the standard carbon fiber specimen as shown in Figure 2 was made first of all. The specimen was subjected to tension until the failure and the results were compared with failure strength of the same specimen made of steel.

The experimental facility adopted is shown in Figure 3. The carbon fiber failure is shown in Figure 4. The results obtained have stated that the carbon fiber specimen has almost eight times higher tensile strength compared with the steel equivalent. The comparison of numerical and experimental results obtained shows a good correspondency of both approaches (see Fig. 5).

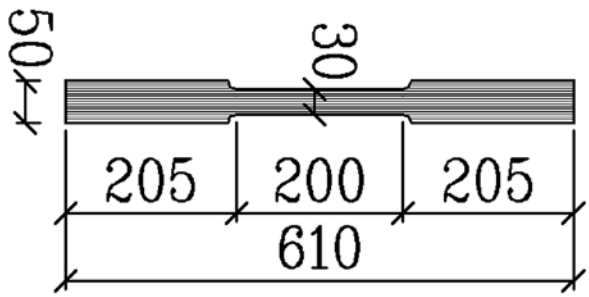

Figure 2. Standard carbon fiber specimen with thickness 1.4 mm

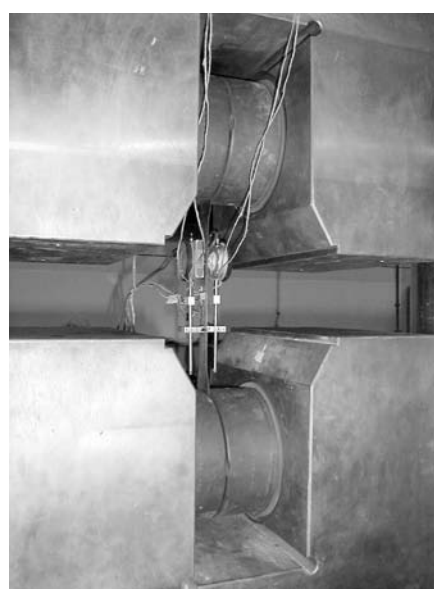

Figure 3. Experimental facility for tensile testing of standard carbon fiber specimen studied

Figure 4. Explosive failure of the standard carbon fiber specimen tested

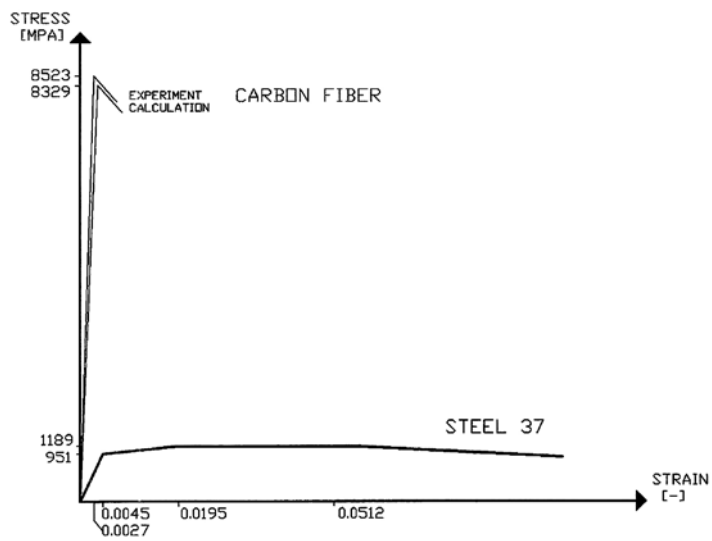

Figure 5. Stress-strain curves of standard specimens studied

5. Applications

The spider-web-like roof made of carbon fiber composites combined with glass elements (see Fig. 6) is studied as an actual application of the above topic. Such a light-weight structure is prone to ultimate wind induced vibrations mentioned as follows:

The wind turbulences force the structure with a considerable power. The forced movements owing to turbulence and associated mechanisms are stochastic in nature.

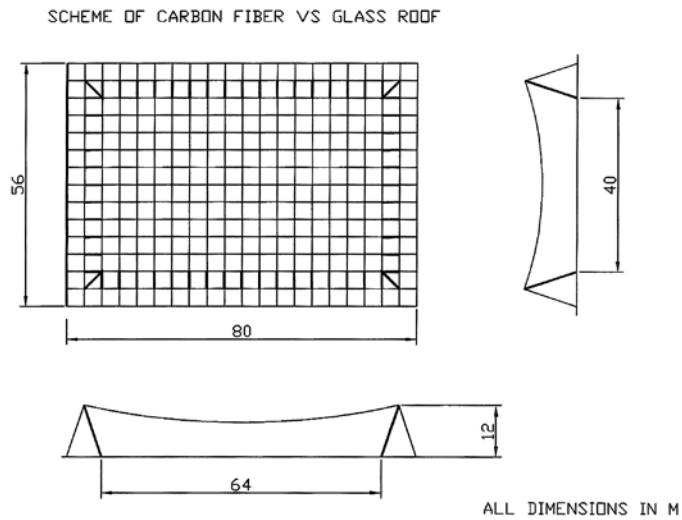

Figure 6. Geometry of slender spider-web-like roof studied

Carbon fiber members can produce a strong vortex wake associated with aerodynamic drag forces appearing. Depending on the wind speed and the cross-section's shape, the shedding of vortices is regular with the periods inversely proportional to the wind speed. In resonance conditions the structure controls the rhythm of the vortex shedding and limited amplitude vibrations appear there. Aside the well known vortex trail type forcing the more general types of aerodynamic excitation mechanism appear there. Possible re-attachment of separated flow, the vortices generated by local shape geometry and by the movement of the structure contribute to periodic aerodynamic forcing.

Aerodynamic forces proportional to the movement of the structure can produce divergent vibrations. In theoretical treatment the concepts of aerodynamic damping and aerodynamic stiffness are to be applied.

In the design of carbon fiber structures it is to be avoided that absolute value of negative aerodynamic damping exceeds the positive mechanical damping producing torsional or flexural mode aerodynamic instability.

At the onset of divergence the critical wind velocity and aerodynamic instability of the structure are initiated.

The time and frequency domain are two frequently used basic approaches for the analysis of aerodynamic response of the structure studied. For the loads changing arbitrarily in time, the first approach aims the solution of convolution type integrals, while the second one involves the Fourier-transformed equations of motion with the frequency as fundamental parameter. For specification of aeroelastic loads in time domain the indicial aerodynamic functions are to be applied.

The advantages of the frequency-domain method of modeling the aeroelastic behaviour of the structure studied are obvious. The flutter derivatives are functions of frequency of vibration and can directly be applied to Fourier-transformed equations of motion given by

$$(-\omega^2 \mathbf{M} + i\,\omega\,\mathbf{C} + \mathbf{K})\,\mathbf{X}(\omega) = [\,i\,\omega\,\mathbf{C}_{Ae}(\omega) + \mathbf{K}_{Ae}(\omega)\,]\,\mathbf{X}(\omega) + \mathbf{F}_b(\omega), \tag{38}$$

where ω is the circular frequency, $\boldsymbol{X}$ and $\boldsymbol{F}_b$ are the vectors of the Fourier transform of nodal degrees of freedom and of nodal dynamic loads, respectively, and it is the imaginary unit. Here, $\boldsymbol{M}$, $\boldsymbol{C}$ and $\boldsymbol{K}$ are the mass, damping and stiffness matrices, respectively, related to the mechanical properties of the structure studied, $\boldsymbol{C}_{Ae}(\omega)$ is the aeroelastic damping matrix and $\boldsymbol{K}_{Ae}$ is the aeroelastic stiffness matrix being defined in the terms of flutter derivatives appearing.

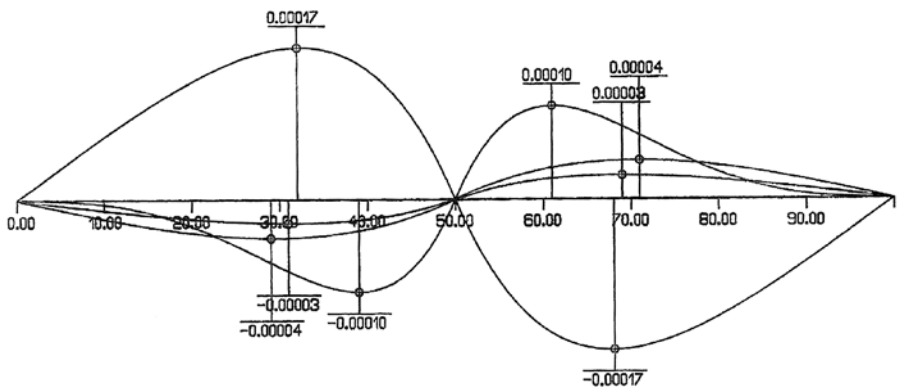

Figure7. Development of ultimate aeroelastic response of the spider-web-like roof studied – antimetric flexural displacements (in m) in nodes 1 – 100 along the length of structure from 1 s (minimal displacement) until 40 s (maximal displacement)

In the structure as shown in Figure 6 the carbon fiber elements were designed as tubes 60/5 mm. The filling members were made as glass plates with thickness 10 mm. As ultimate behaviour there was tested the development of antimetric flexural displacements into aeroelastic ultimate response of the structure subjected to the laminar wind action with speed 30 m/sec and with pressure 1.0 MN/m^2. The structural response obtained is plotted in Figure 7. Another results obtained are submitted, for example, in references (Tesar and Simoncic, 2002) and (Tesar, Sotakova and Minar, 2002).

Conclusions

The analysis and numerical as well as experimental results sampled up submit an image of the ultimate response of structures made of carbon fiber composites. The analysis of material instability with adoption of the fiber kinking theory for the study of the failure process resulted in the approximations for the problem treatment. The micromechanical analysis performed is based on the discrete simulation of the problem in space, time and temperature. Some results with an actual application are submitted.

Acknowledgements

The author is indebted to the Slovak Grant Agencies VEGA and APVV for supporting the above research.

References

[1] Simo, J. C. (1987), "On a fully three-dimensional finite strain viscoelastic damage model – formulation and computational aspects", Computer Methods in Applied Mechanics and Engineering 60, 153-173.
[2] Tesar, A. and Fillo, L. (1988), Transfer Matrix Method, KLUWER Academic Publishers, Dordrecht/Boston/London.
[3] Tesar, A. and Svolik, J. (1993), "Wave distribution in fibre members subjected to kinematic forcing", Int. Journal for Communication in Numerical Mechanics 9, 189-196.
[4] Budiansky, B. (1983), "Micromechanics", Computers Structures", Vol. 16, 3-12.
[5] Duk-Hyun, Kim (2002), Composite Structures for Civil and Architectural Engineering, Taylor & Francis.
[6] Extren Design Manual, Strongwell Corporation, Bristol, Virginia, 1998.
[7] Tesar, A. and Simoncic, M. (2002), "Fatigue behaviour of tghin-walled fiber-glass composites" Building Research Journal 50, 35-48.
[8] Tesar, A., Sotakova, D. and Minar, M. (2002), "Micromechanics of fibre glass composites at elevated temperatures", Int. Journal for Numerical Methods in Engineering, 55, 317-338.